NASA TECHNICAL MEMORANDUM

NASA TM X-52652

NASA TM X-52652

SIMILARITY AND CURVATURE EFFECTS IN POOL FILM BOILING

by Robert C. Hendricks and Kenneth J. Baumeister
Lewis Research Center
Cleveland, Ohio

TECHNICAL PAPER proposed for presentation at
Fourth International Heat Transfer Conference
Versailles/Paris, August 31-September 5, 1970

SIMILARITY AND CURVATURE EFFECTS IN POOL FILM BOILING

by Robert C. Hendricks and Kenneth J. Baumeister

Lewis Research Center
Cleveland, Ohio

TECHNICAL PAPER proposed for presentation at

Fourth International Heat Transfer Conference
Versailles/Paris, France, August 31-September 5, 1970

NATIONAL AERONAUTICS AND SPACE ADMINISTRATION

SIMILARITY AND CURVATURE EFFECTS IN POOL FILM BOILING

by Robert C. Hendricks and Kenneth J. Baumeister
NASA Lewis Research Center, Cleveland, Ohio

Abstract

Cooldown film-boiling-heat transfer data from small diameter spheres (0.0397 to 1.27 cm) are presented, and the effects of curvature and similarities of the theoretical analyses for the flat plate, cylinder, and sphere are assessed. The data are in good agreement with theory but are significantly higher than predicted from the classic Bromley equation.

INTRODUCTION

Film-boiling heat transfer from small diameter spheres is of fundamental interest in studying the effects of curvature, and of practical importance in engineering and biology. In nuclear reactors, small fission fragments (approximated by a sphere) can get "loose" and film boil in the coolant passages producing voids. In preservation of biological specimens and human organisms, the heat transfer rates of small, fluid globules must be accurately known to control the freezing process.

Film boiling heat transfer to a flat plate or a surface with no curvature has been studied by several authors (e.g., 1,2), and the fundamental relation presented by Berenson (Ref. 1)

$$Nu_\ell = 0.424(Ra^*_\ell)^{1/4}$$

correlated much of the available data. Film boiling from a cylinder (single curved surface) has also been studied by several authors (e.g., 3,4). Extending the previous work, Breen and Westwater (Ref. 4) empirically correlated much of the available cylinder data

$$Nu_\ell = (0.069\lambda_c/d + 0.59)(Ra^*_\ell \ell/\lambda_c)^{1/4}$$

Compared with the classic Bromley correlation, $\left[Nu_d = 0.62(Ra^*_d)^{1/4}\right]$, ref. 3, this correlation predicts a significant increase in heat transfer for very small and very large diameter cylinders. Later, Baumeister and Hamill (Ref. 5) analyzed film boiling from the flat plate and the cylinder and were able to correlate available data. Their model extended the understanding of the film boiling process.

Film boiling from a sphere has been studied by references 6, 7, 8, 9, and 10. The analysis of Frederking and Clark (Ref. 10) correlates much of the available data for large-diameter spheres.

$$Nu_d = 0.14\ Ra^{*1/3}_d$$

Recently, Hendricks and Baumeister (Ref. 7) analyzed film boiling from both small and large spheres and were also able to correlate these data. However, a significant difference exists in the correlations for the small-sphere case. Thus the pur-

pose of this paper is to present experimental film-boiling heat transfer data for small spheres, test the analysis of reference 7, and also to assess the effects of curvature and similarities of the theoretical analysis for the flat plate, cylinder, and sphere. The analyses are outlined in the Appendix and the results given in table I.

APPARATUS AND PROCEDURE

Cool down heat transfer data were taken on six different spheres with diameters ranging from 0.0397 to 1.27 cm. In each experiment, room temperature spheres were quenched in a bath of liquid nitrogen.

The smallest spheres (0.0397 and 0.0794 cm) were Tungsten-Carbide while the four remaining larger spheres (0.1585; 0.318; 0.397; and 1.27 cm) were copper. Tungsten Carbide was the only commerically available material for the small diameter spheres. The 0.0397, 0.0794, 0.1585, and 0.397 cm spheres were instrumented with 0.00126 cm diameter Chromel-Alumel thermocouple; while the 0.318 and 1.27 cm spheres had none. The heat transfer to the uninstrumented spheres was evaluated by measuring the quenching time (discussed in detail later). The couples were spot welded to the Tungsten-Carbide spheres and embedded into the copper spheres. The thermocouple output was recorded and reduced; a typical plot is shown in Figure 1. The accuracy of the recording system was within $\pm 3^{\circ}$ K and the reproducibility of the data was within ±10%.

In Figure 1, t_{Leid}, represents the time for film boiling to cease, while t_Q, represents the time required for the sphere to reach the bath temperature. A sharp break in the time temperature curve can be seen in Figure 1 at t_{Leid}, and condition (1) follows:

$$t_{Leid} \approx t_Q \tag{1}$$

The measurement of t_Q will be shown to give a good first order estimate of the heat transfer coefficient. For the noninstrumented spheres, the quenching time was measured using a 1/100 second stopclock and coordinated visually. Each sphere was quenched ten times and an average time was taken. The deviation ranged from ±15% for the 0.0397 cm sphere to less than 1% for the 1.27 cm diameter sphere.

THERMOMETRY ERROR

The thermocouple conduction errors in measured surface temperature were estimated by modifying the analysis of reference 11, and found to be less than 1° K; no correction was applied to the data.

The sensible heat loss by conduction through the thermocouple wires was estimated using the cylindrical fin equation

$$q_{TC} = 2\pi r_\omega \sqrt{2h_L k_e r_\omega}\,(T_w - T_s) = 2\pi r_\omega \sqrt{k_e k_L Nu_L}\,(T_w - T_s) \tag{2}$$

In these calculations, values of $k_e = 0.044$ cal/cm-sec-K and $Nu_L = 1$ were assumed and q_{TC} altered the heat transfer coefficient as much as 25% for the 0.0397 cm sphere.

EXPERIMENTAL HEAT TRANSFER COEFFICIENT

The energy equation for quenching a sphere is given as

$$-\rho c V D_t(T_W - T_S) = hA(T_W - T_S) + q_{TC} \tag{3}$$

where the bath is at the saturation liquid temperature T_S. At any instant the thermal capacitance (ρcV) and the wall temperature T_W are assumed uniform throughout the sphere. The latter assumption is justified because the value of the Biot modulus ($B_i = hd/k$) is low. By rearranging equation (3), the film boiling heat transfer coefficient can be expressed as

$$h = -(\rho cV/A)D_t \ln(T_W - T_S) - q_{TC}/A(T_W - T_S) \tag{4}$$

Since the geometry and properties are known, the heat transfer coefficients were determined directly from equation (4) using values of $D_t \ln(T_W - T_S)$ from the experimental data of Figure 1. The results are illustrated in Figure 2. For the 0.0397 and 0.0797 cm spheres two heat transfer paths were found. The reason for these paths is at present unknown, and attributed to uncertainities in the data.

Average Heat Transfer Coefficient

As seen in Figure 2, for $\Delta T > 90^{\circ}$ K the heat transfer coefficients are reasonably constant. Consequently, assuming average properties and neglecting heat losses, an average heat transfer coefficient is found by solving equation (3). This gives

$$(T_W - T_S)/T_{W_o} - T_S) = \exp(-t/\tau_c) = \exp(-thA/\rho cV) \tag{5}$$

where T_{W_o} is the initial sphere temperature and τ_c is the sphere time constant. For a given thermal resistance ($1/hA$) and capacity (ρcV), the system time constant τ_c can be specified. To determine τ_c, the average heat transfer coefficient, $\bar{h}$, was estimated from the data in reference 8. Assuming condition (1), the quench-time to the calculated-time-constant ratio t_Q/τ_c was experimentally found to be 1.85; consequently a first-order estimate of the average heat-transfer coefficient can be made

$$\bar{h}_\gamma = (\rho cd/\epsilon)/(t_Q/1.85) \tag{6}$$

Without any attached instrumentation, simply observing the quenching time, equation (6) gave values for the heat transfer coefficient which were in good agreement with the values determined from equation (4).

DISCUSSION OF THEORETICAL AND EXPERIMENTAL RESULTS

In the derivation of the heat-transfer coefficients outlined in the Appendix, the heat transfer coefficients (listed in table I) are found to be a function of two key similarity parameters ℓ and Bond number B_o. The theoretical expressions for Nusselt number are plotted as a function of Bond number in Figure 3 for the flat plate, cylinder, and sphere along with the classical Bromley equation. As is evident, at low Bond number a significant enhancement in heat transfer due to curvature is predicted for

both the cylinder and the sphere. Using these same parameters, the experimental heat-transfer data for spheres are compared with theory in Figure 4.

It is apparent that the data significantly depart from the large sphere analysis of reference 10 as well as the classic Bromley relation and follow those trends established in Figure 3. However, while the analysis of reference 7 predicts the general data trend, the 0.0397 cm sphere data appear on the average to be about 25% higher than theory. Three factors which may contribute to this deviation are: (1) difficulties in assessing large time-temperature gradients, (2) significant heat loss through the thermocouple, and (3) uncertainty in the heat transfer data as illustrated in Figure 2 and the specific heat of tungsten carbide. The vertical scatter in the data of Figure 3 exhibits a dependence on temperature difference which is not accounted for by the theory. (This is also true for the flat plate and the cylinder.) Perhaps a variable property analysis would encompass these trends. In addition, data for a 10.16 cm diameter sphere (Ref. 8) and those collected in reference 7 are in agreement with the theory as seen in Figure 4. These data verify the theory for a Bond number range from 0.132 to 8700.

SIMILARITY

Similarities exist between the flat plate, cylinder, and sphere in the method of modeling, governing equations, boundary conditions, constraints, and evolved similarity parameters. Sufficiently allied are these criteria as to suggest they form a solution basis for all pool film boiling problems (see Appendix for details).

Some physical similarities between the sphere and cylinder are noted in Figure 5. At small B_o, the vapor release is periodic and the field quiescent. The transition regimes are similar and note the analogous chaotic appearance at large B_o. Figure 6 shows the similar idealized vapor dome configurations chosen to model the phenomena. The vapor dome spacing parameter λ is related through hydrodynamic stability theory to B_o.

CONCLUSIONS

(1) The theoretical analysis of reference 7 predicted a significant increase in the film-boiling heat-transfer coefficient for small-diameter spheres, compared with previous analysis for large-diameter spheres. Experimental film boiling data for small spheres ranging from 0.0397 to 1.27 cm confirm the theoretical prediction.

(2) The Bond number is shown to be a key correlating parameter in relating the enhancing effect of system curvature on the film boiling heat transfer coefficient. This enhancement becomes extremely pronounced at small Bond numbers (small spheres or cylinders) and approaches that of the flat plate at large Bond numbers. Equivalently, if the radii of curvature are small, or very large, compared with the vapor dome spacing parameter ℓ, the effects of curvature augment the heat transfer over that predicted by the Bromley relation.

REFERENCES

(1) P. J. Berenson: Film-Boiling Heat Transfer From a Horizontal Surface. J. Heat Transfer, vol. 83, No. 3, pp. 351-358 (Aug. 1961).

(2) T. D. Hamill and K. J. Baumeister: Effect of Subcooling and Radiation on Film-Boiling Heat Transfer From a Flat Plate. NASA TN D-3925 (Aug. 1967).

(3) L. A. Bromley: Heat Transfer in Stable Film Boiling. Chem. Eng. Prog., vol. 46, No. 5, pp. 221-224 (May 1950).

(4) B. J. Breen and J. W. Westwater: Effect of Diameter of Horizontal Tubes on Film Boiling Heat Transfer. Chem. Eng. Prog., vol. 58, No. 7, pp. 67-72 (July 1962).

(5) K. J. Baumeister and T. D. Hamill: Laminar Flow Analysis of Film Boiling From a Horizontal Wire. NASA TN D-4035 (1967).

(6) T. H. K. Frederking, R. C. Chapman, and S. Wang: Heat Transport and Fluid Motion During Cooldown of Single Bodies to Low Temperatures. Inter. Adv. in Cryogenic Engineering, vol. 10, K. D. Timmerhaus, ed., Plenum Press, pp. 353-360 (1965).

(7) R. C. Hendricks and K. J. Baumeister: Film Boiling From Submerged Spheres. NASA TN D-5124 (June 1969).

(8) L. Manson: Cooldown of Shrouded Spherical Vessels in Liquid Nitrogen. Adv. in Cryogenic Engineering, vol. 12, K. D. Timmerhaus, ed., Plenum Press, pp. 373-380 (1967).

(9) L. G. Rhea: Boiling Heat Transfer From an Oscillating Sphere With a Cryogenic Fluid at Atmospheric Pressure and Standard Gravity. Ph.D. Thesis, Kansas State University (1967).

(10) T. H. K. Frederking and J. A. Clark: Natural Connection Film Boiling on a Sphere. Adv. in Cryogenic Engineering, vol. 8, K. D. Timmerhaus, ed., Plenum Press, pp. 501-506 (1963).

(11) L. M. K. Boelter, F. E. Romie, A. G. Guibert, and M. A. Miller: An Investigation of Aircraft Heaters. XXVII - Equations for Steady-State Temperature Distribution Caused by Thermal Sources in Flat Plates Applied to Calculation of Thermocouple Errors, Heat-Meter Corrections, and Heat Transfer by Pin-Fin Plates. NACA TN D-1452 (August 1948).

APPENDIX A

General Method of Solution

The method of modeling and the theoretical solutions for film boiling from the flat plate, cylinder, and sphere are quite similar. In this Appendix we shall review the models, the governing equations, their solutions and seek similarity forms which will enable us to compare the effects of curvature on the film boiling process.

Consider the models of film boiling from the horizontal flat plate, horizontal cylinder,

and sphere as shown in Figure 6. As seen in Figure 6, a thin vapor gap thickness δ and vapor dome are common to all the geometries. In all cases, the liquid evaporates and flows into domes which are assumed to form in a temporal periodic manner at regular intervals λ or θ^*. One coordinate is eliminated through geometric symmetry thereby enabling one to employ the stream function in solving the momentum equations.

Basic Assumptions

For all geometries, the creeping flow assumptions are made, the gap thickness is taken as constant, and surface capillary waves, while influencing the boundary, do not significantly alter the heat transfer or the laminar nature of the flow. In considering the energy transport, radiation is neglected, the properties are evaluated at the film temperature ($T_f = (T_w + T_s)/2$), and convective terms are neglected in comparison with the conductive terms in the energy equation. The convective term in the last assumption are usually accounted for by replacing the latent heat of vaporization with a modified heat of vaporization of the form

$$\lambda^* = \lambda_1(1 + \tfrac{1}{2} C_p \Delta T/\lambda_1) \tag{7}$$

Justification for these assumptions is given in references 2, 5, and 7.

Governing Equations and Boundary Condition

With the previous assumptions the governing momentum and energy equations can be written as

$$E^4\psi = 0; \qquad \nabla^2 T = 0 \tag{8}$$

The operators E^4 and ∇^2 are given in references 2, 5, and 7 for each of the three coordinate systems under consideration, that is, for the flat plate, cylinder and sphere geometries. Reference 2 also presents a solution of equation (8) with a convective term left in the equation, resulting in a modified latent heat of vaporization, similar to equation (7).

For the boundary conditions, the tangential vapor velocity to the interface is assumed to be zero, the interface to be at constant temperature T_s, and the wall at a constant temperature T_w. Also, uniform vaporization is assumed at the liquid-vapor interface and, of course, zero velocity at the heater surface.

Constraints

The above assumptions and boundary conditions do not lead to a tractable problem because the vapor gap thickness, interface velocity, and vapor dome spacing are unknowns. Thus, three additional constraints are required.

(1) Static Force Balance Constraint. - The average pressure $\overline{P}_s$ on the vapor side of the liquid vapor interface results from the weight of the supported liquid, ambient pressure, and surface tension effects. This average pressure, $\overline{P}_s$, must be balanced by the vapor pressure field arising from the flow of vapor into the vapor dome

$$\int_A P_I \, dA = \bar{P}_g A \tag{9}$$

where P_I is the pressure evaluated at the liquid-vapor interface.

From this balance arises the two similarity parameters ℓ and B_o, discussed in the body of the report.

(2) Interface Energy Balance Constraint. - The energy conducted across the vapor gap vaporizes the liquid and a balance must be maintained between the advancing evaporating interface and the incident energy. The energy balance may be written as

$$-\rho\lambda u_\delta = q = -k \, \partial T/\partial n \Big|_I \tag{10}$$

where n represents the coordinate normal to the interface. In reference 2, the balance is augmented to include the effects of subcooling and radiation.

(3) Optimization Constraint. - In determining the vapor dome spacing parameters, the energy transfer or rate of entropy production is assumed to be a maximum

$$\partial \bar{h}_w/\partial L = 0; \; \partial^2 \bar{h}_w/\partial L^2 < 0 \tag{11}$$

where L represents a characteristic wavelength or dome spacing parameter and $\bar{h}_w$ is the area weighted heat transfer coefficient:

$$\bar{h}_w = h_{fb}(A_{fb}/A_T) + h_D(A_D/A_T) \tag{12}$$

The hypothesis asserts that the characteristic wavelength adjusts the size and spacing of the vapor dome to optimize the rate of heat removal from the surface. The wavelengths predicted by this assumption compare favorably with the experimental data.

With these three constraints, the system is now determinant. The analytical solutions are listed in table I and shown in Figure 3 along with the general solution; Table I also shows some special limiting cases.

Heat Transfer Similarities

The solutions for the horizontal flat plate (Ref. 2), cylinder (Ref. 5), and the sphere (Ref. 7) are presented in table I in terms of Rayleigh numbers defined as,

$$R^*_{a_d} = \rho(\rho_L - \rho)g\lambda^* \, d^3/(k\mu \, \Delta T) \tag{13}$$

$$R^*_{a_\ell} = \rho(\rho_L - p)g\lambda^* \, \ell^3/(k\mu \, \Delta T) \tag{14}$$

The flat plate represents the limiting case of a surface with no curvature, while the horizontal cylinder has one finite curvature. Except for the slight difference in the constants of proportionality (0.424 compared with 0.373) the finite curvature of the wire increases the heat transfer by a factor

$$\left[1 + 9\Big/\sqrt{6B_o} + 8\Big/\left(3\sqrt{(6B_o)^3}\right)\right]^{1/4} \tag{15}$$

For small cylinders (small Bond numbers, B_o) the heat transfer coefficient will be significantly affected by the curvature of the surface, likewise for the sphere. Figure 3 illustrates this quite graphically. At small Bond numbers, figures 3 and 4 show that the heat transfer coefficient from the sphere will be greater than that from an equivalent cylinder because the second component of curvature on the sphere further enhances the heat transfer.

NOMENCLATURE

A	area
B_o	Bond number $(d/\ell)^2$
C_p	specific heat at constant pressure
c	specific heat
d	diameter
D_t	derivative with respect to time
E^4	differential operator
$G(B_o)$	function defined in reference 7
g	local acceleration
g_c	gravitational conversion constant
h	heat transfer coefficient
k	thermal conductivity
k_e	effective thermocouple thermal conductivity, $\frac{1}{2}\left(\sqrt{k_{\omega_1}} + \sqrt{k_{\omega_2}}\right)$
ℓ	dome spacing parameter, $\sqrt{\sigma g_c/(\rho_L - \rho)g}$
L	characterizing length
Nu	Nusselt number
P	pressure
q	heat flux
r	radius
R_o	radius of sphere
Ra*	modified Rayleigh number (Eq. (13))
t	time
t_Q	quenching time
T	temperature
ΔT	temperature difference $(T_w - T_s)$
u, v	velocity components
V	volume
δ	vapor gap thickness
ρ	density
σ	surface tension
ψ	stream function
θ^*	reference angle (Fig. 6) - values tabulated in ref. 7
λ^*	modified latent heat of vaporization (eq. (11))
λ_1	latent heat
λ_c	characteristic wavelength
λ	wavelength
τ_c	system time constant
μ	viscosity

Subscripts:

d	diameter
D	vapor dome
f	film conditions
fb	film boiling
I	interface
ℓ	based on characteristic length
L	liquid
Leid	Leidenfrost
s	saturation
T	total
w	surface or wall
w_o	initial surface or wall
ω	wire (thermocouple)
δ	evaporating interface
γ	average, uninstrumented

Table I. - Theoretical Heat Transfer Expressions and Limiting Cases for Three Geometries, The Flat Plate, Cylinder, and Sphere

Nusselt number expression	Limiting cases
Horizontal Flat Plate $Nu_\ell = \frac{h\ell}{k} = 0.424(Ra_\ell^*)^{1/4}$	A special limit in itself
Horizontal Cylinder $Nu_d = \frac{hd}{k} = 0.373(Ra_d^* \sqrt{B_o})^{1/4}\left[1 + \frac{9}{\sqrt{6B_o}} + \frac{8}{3\sqrt{(6B_o)^3}}\right]^{1/4}$	Large B_o $Nu_d = 0.373(Ra_d^*\sqrt{B_o})^{1/4}$ Small B_o $Nu_d = 0.00846\left(\frac{Ra_d^*}{B_o}\right)^{1/4}$
Sphere $Nu_d = 2 + \frac{1}{4}\left[\frac{-2Ra_d^* G(B_o)}{3}\right]^{1/4} + \left[0.177(Ra_d^*\sqrt{B_o})^{1/4} + \csc\theta^*\right](1 + \cos\theta^*)$	Large B_o $Nu_d = 0.35(Ra_d^*\sqrt{B_o})^{1/4}$ Small B_o $Nu_d = 3 + (Ra_d^*\sqrt{B_o})^{1/4} \times \left[\frac{0.71}{B_o^{1/8}} + 0.177\right]$

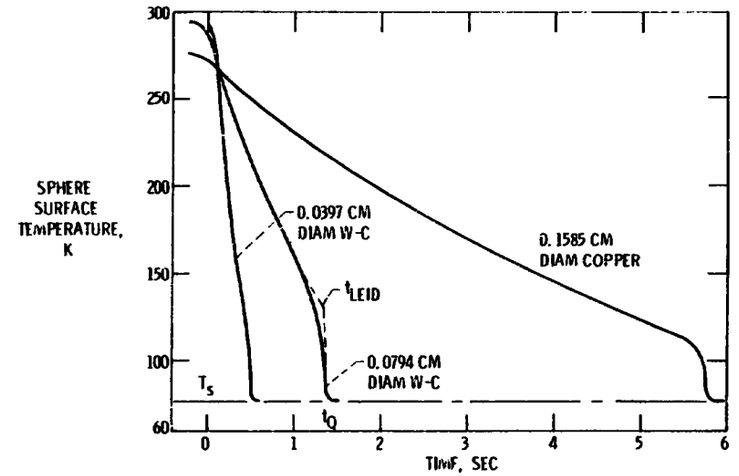

Figure 1. - Typical time-temperature histories for cooldown of spheres in saturated liquid nitrogen.

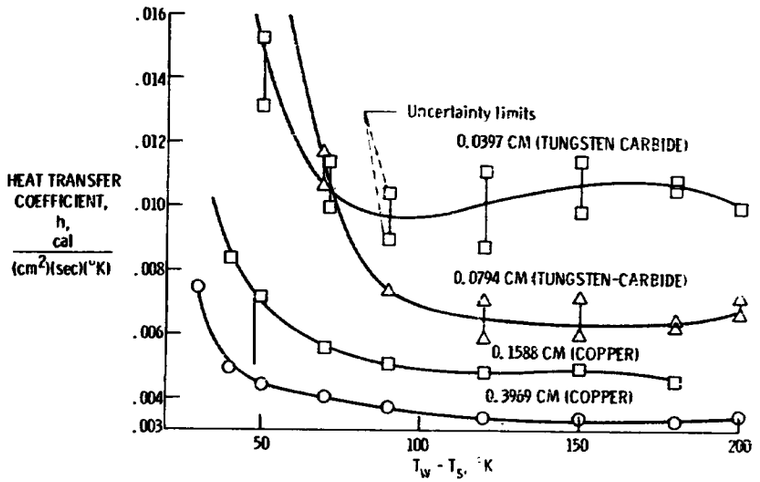

Figure 2. - Heat transfer coefficient as a function of temperature difference for four spheres.

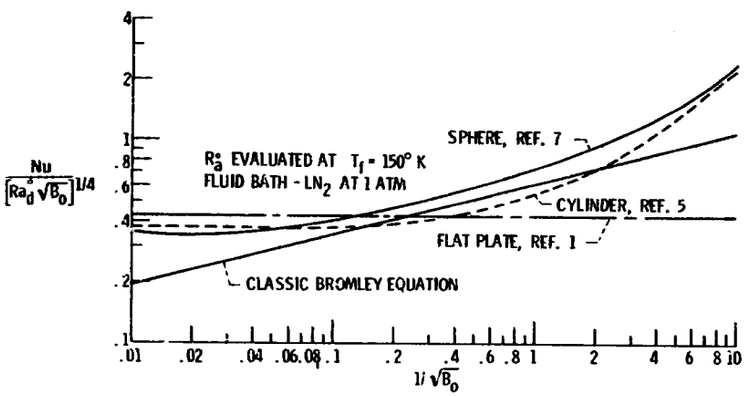

Figure 3. - Theoretical comparison of curvature effects on pool film boiling for the flat plate, cylinder, and sphere. The classic Bromley equation is for reference.

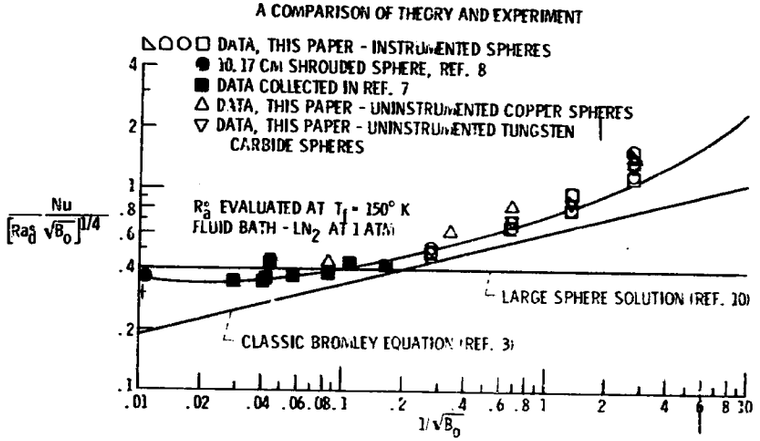

Figure 4. - Film boiling heat transfer data for spheres.

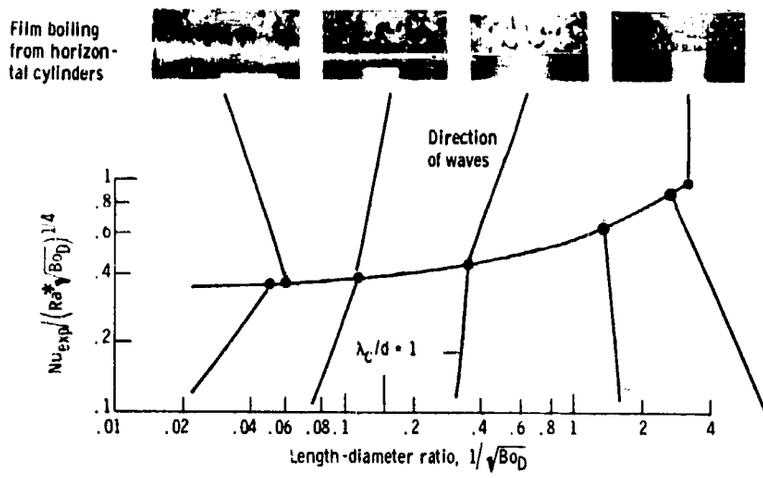

Figure 5. - Effect of geometry and Bond number for film boiling off curved surfaces, in liquid nitrogen.

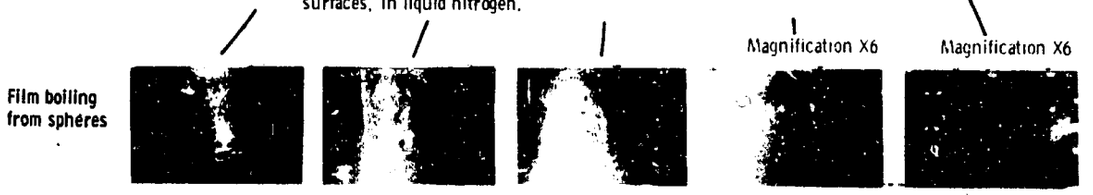

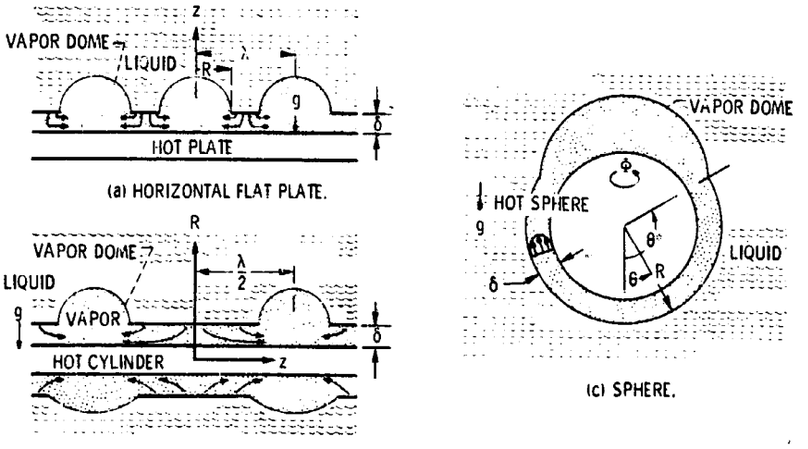

Figure 6. - Idealized model of film boiling from various geometries.